Supporting Information

Self-discharge mechanism of high voltage $KVPO_4F$ for K-ion batteries

Romain Wernert[†‡Δ], Long H.B. Nguyen[†‡Δ], Antonella Iadecola[Δ], François Weill[†Δ||], François Fauth[§], Laure Monconduit[‡Δ||], Dany Carlier[†Δ||*], Laurence Croguennec[†Δ||*]

AUTHOR ADDRESS

† Univ. Bordeaux, CNRS, Bordeaux INP, ICMCB, UMR 5026, F-33600 Pessac, France

‡ ICGM, Univ. Montpellier, CNRS, ENSCM, 34095 Montpellier, France

Δ RS2E, Réseau Français sur le Stockage Electrochimique de l'Energie, FR CNRS #3459, Amiens F-80039 Cedex 1, France

§ CELLS-ALBA synchrotron, E-08290, Cerdanyola del Vallès, Barcelona, Spain

|| ALISTORE-ERI European Research Institute, FR CNRS 3104, F-80039 Amiens Cedex 1, France

***Corresponding authors:**
Dany Carlier: dany.carlier@icmcb.cnrs.fr
Laurence Croguennec: laurence.croguennec@icmcb.cnrs.fr

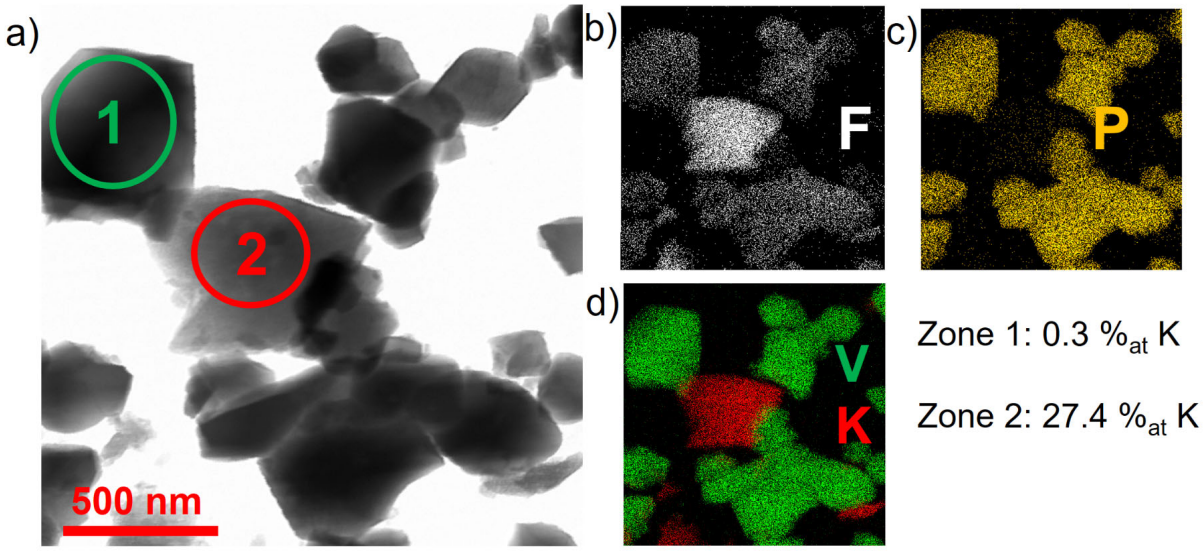

Figure S1: EDX mapping of the sample obtained after chemical deintercalation $KVPO_4F$: a) STEM image, b) EDX mapping of F, c) EDX mapping of P, d) EDX mapping of V (in green) and K (in red).

Table S1: Atomic parameters and first neighbour interatomic distances of K_0VPO_4F refined by the Rietveld method.

K_0VPO_4F		**Pnan**	Z=8	ρ = 2.75 g/cm^3		
		a (Å) 12.504(1)	b (Å) 6.0875(5)	c (Å) 10.462(1)		
	Wyckoff position	x/a	y/b	z/c	occupancy	B_{iso} (Å^2)
$V2_{trans}$	4a	0	0	0	1	1.0(1)
$V1_{cis}$	4d	0.145(1)	¼	¾	1	1.2(2)
P1	4c	¼	0.070(2)	0	1	1.3(2)
P2	4d	-0.062(1)	¼	¼	1	1.3(2)
O1a	8e	0.246(2)	0.230(4)	-0.116(2)	1	1.2(2)
O2a	8e	0.149(1)	-0.067(2)	0.010(3)	1	1.2(2)
O1b	8e	-0.133(2)	0.051(4)	0.274(2)	1	1.2(2)
O2b	8e	0.010(2)	0.294(5)	0.367(2)	1	1.2(2)
F1	8e	0.028(2)	0.277(5)	0.626(2)	1	1.2(5)

Bond	Distance (Å)*	Bond	Distance (Å)*
V2−O2a	1.90 × 2	V1−O1a	1.90 × 2
V2−O2b	1.88 × 2	V1−O1b	1.85 × 2
V2−F1	1.93 × 2	V1−F1	1.95 × 2
P1−O1a	1.55 × 2	P2−O1b	1.53 × 2
P1−O2a	1.53 × 2	P2−O2b	1.54 × 2
	$V1(O_4F_2)$	$V2(O_4F_2)$	
Site distortion (10^{-4})	17.2	4.4	

*rounded to 10^{-2} Å

The site distortion depicts the deviation from a regular octahedron and was calculated using the following formula:

$$\Delta = \frac{1}{6}\sum_{i=1}^{6}\frac{(d_i-\bar{d})^2}{\bar{d}^2}$$

Where d_i corresponds to each V−X bond of the octahedron and $\bar{d}$ is the average bond length.

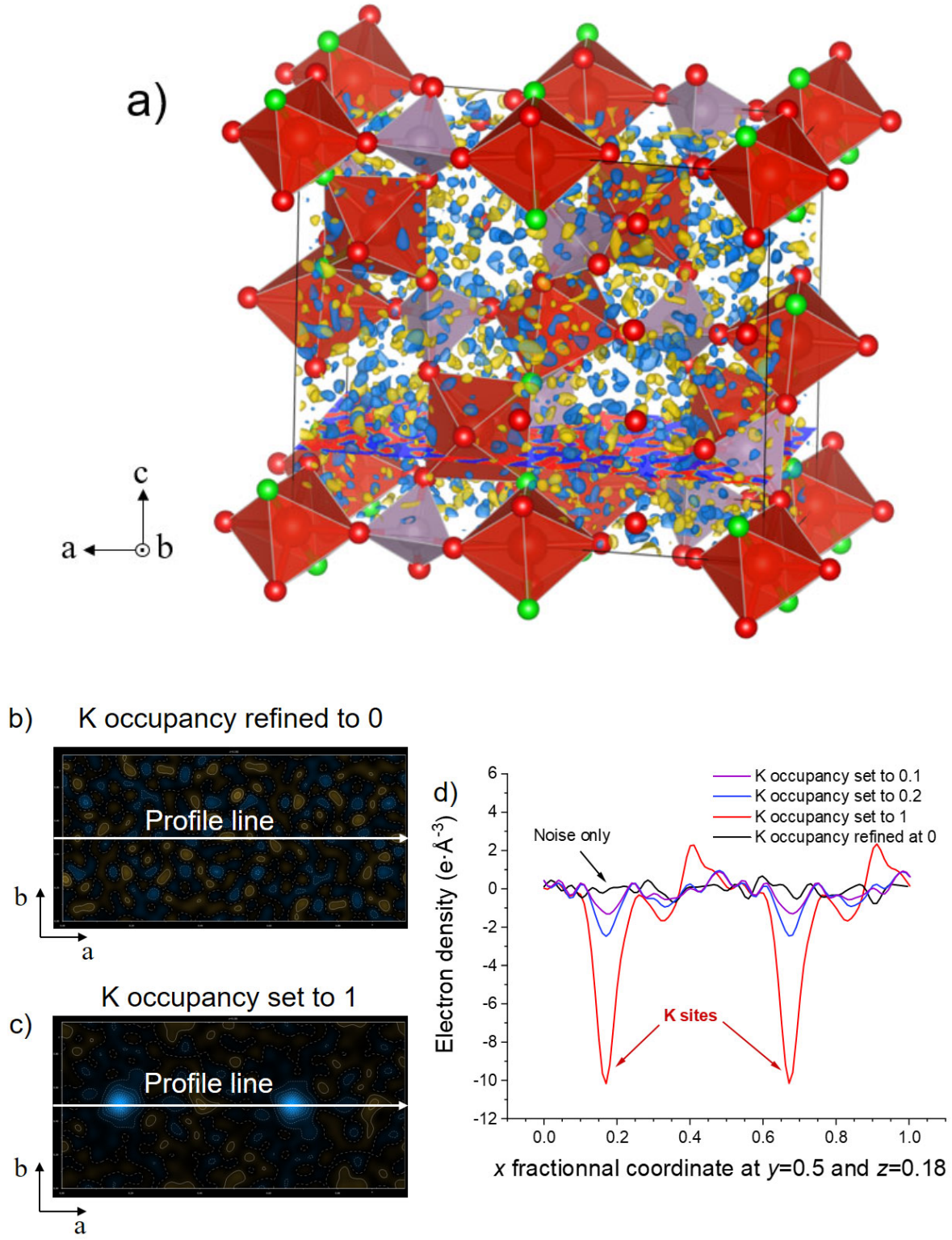

Figure S2: a) Isosurface Fourier difference map calculated from the Rietveld refinement of K_0VPO_4F drawn in 3D at isosurface 0.7 e·Å^{-3}. Negative electron densities are drawn in blue and positive in yellow. The slice in the (x,y) plane at z= 0.18 is represented for the case of K occupancy being refined (b) and K occupancy being set to 0.1, 0.2 or 1 (c). d) The comparison between both Fourier difference maps and profile line along x for y = 0.5 and z = 0.18 shows absolutely no residue, indicating the full deintercaltion of K sites.

Table S2: Comparison of experimental (SXRD) and calculated cell parameters for K_0VPO_4F.

	a (Å)	b (Å)	c (Å)	V/Z (Å^3)
Exp	12.504(1)	6.0875(5)	10.462(1)	99.544(3)
GGA+3eV	12.688	6.173	10.642	104.18
GGA+5eV	12.706	6.199	10.675	104.95

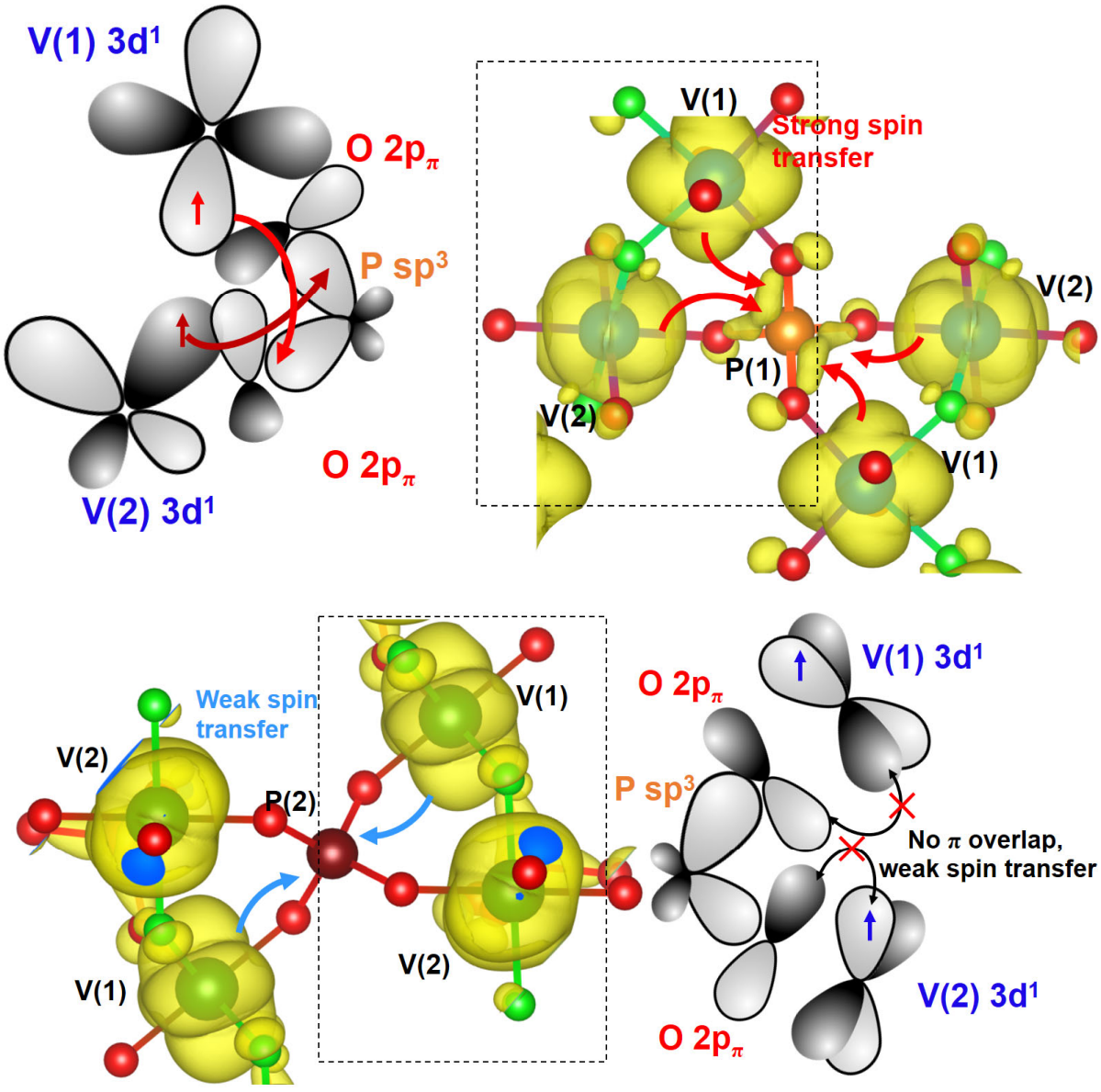

Figure S3: Spin density maps around P(1) (top) and P(2) (bottom) crystallographic sites with isosurface 10^{-3} spin·Å^{-3} calculated with U_{eff} = 5 eV. The spin transfer mechanism is depicted with orbital schematic.

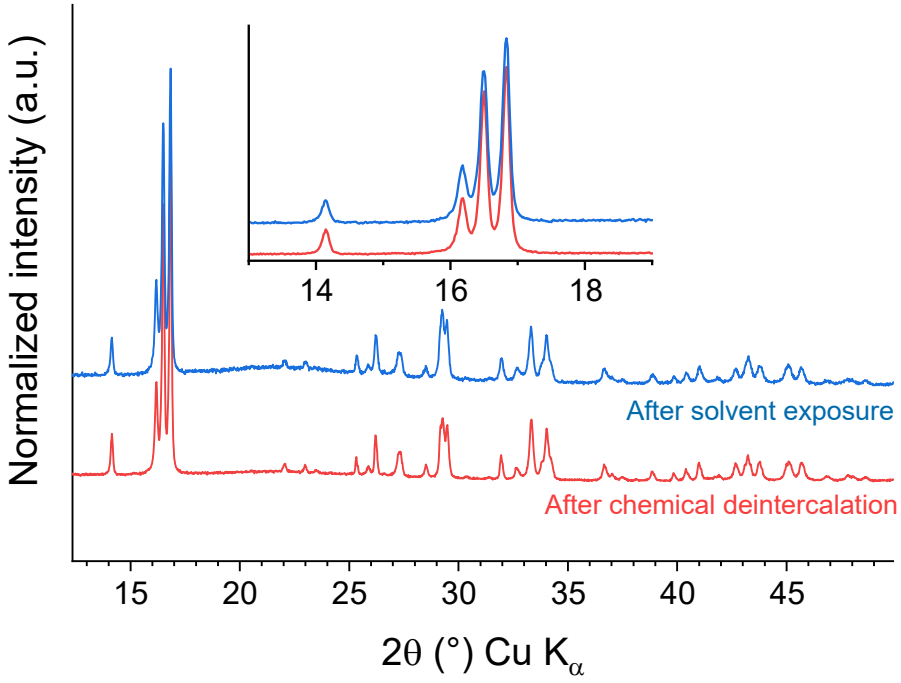

Figure S4: XRD patterns of K_0VPO_4F before and after solvent exposure.

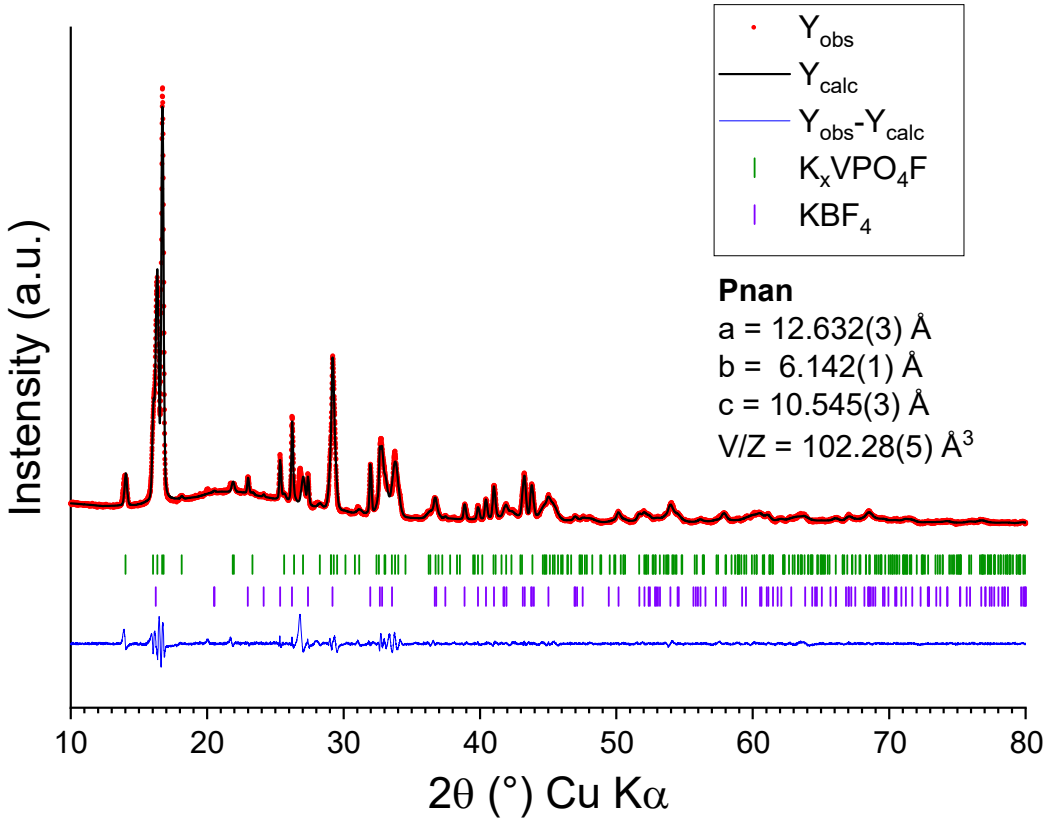

Figure S5: Two phases Lebail refinement of the compound recovered after immersion of K_0VPO_4F in the electrolyte (K_xVPO_4F + KBF_4). The unit cell volume of K_xVPO_4F has expended by 2.8% compared to K_0VPO_4F

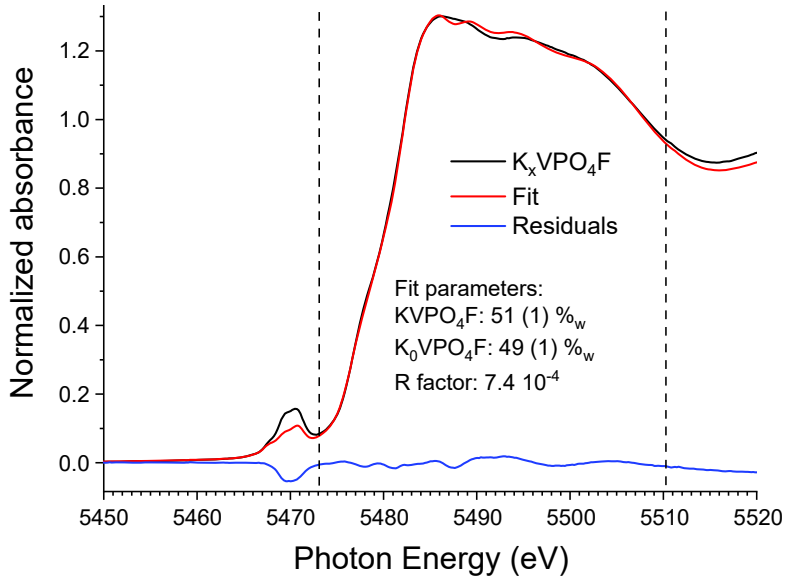

Figure S6: Linear combination fitting of the V K-edge of K_xVPO_4F using the spectra of $KVPO_4F$ and K_0VPO_4F as standards.

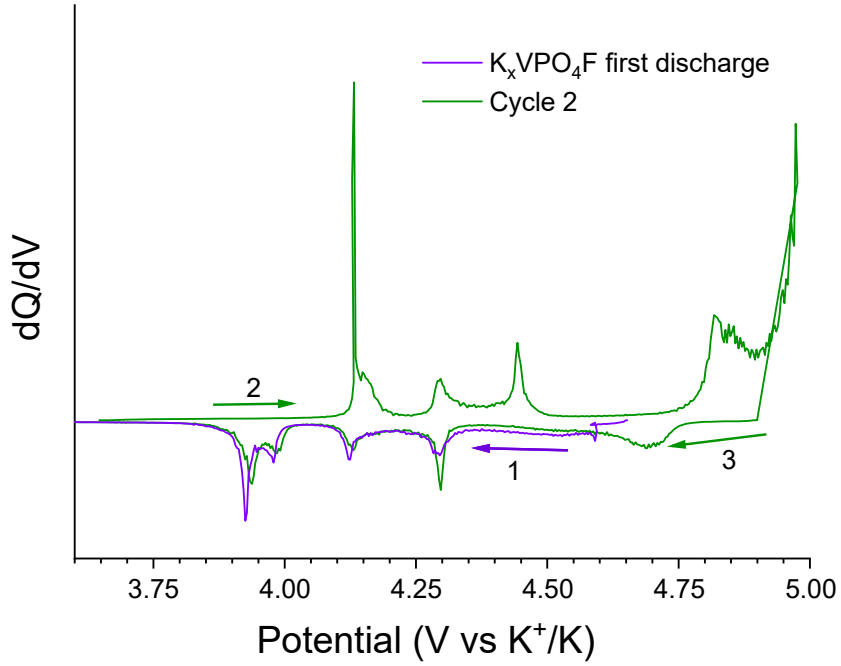

Figure S7: Derivative plot of galvanostatic cycling curves of K_xVPO_4F versus K metal at C/20.

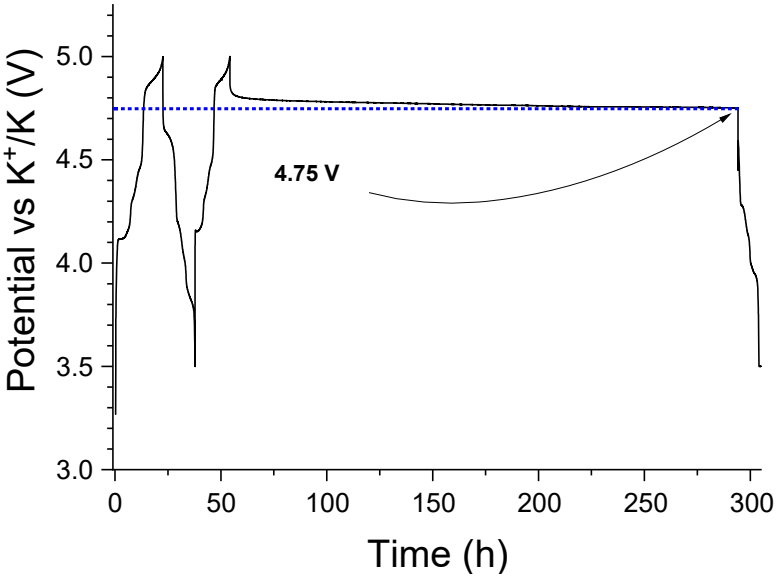

Figure S8: Potential versus time plot of the 10 days OCV (after the second charge) to measure the corresponding self-discharge for $KVPO_4F$ versus K metal when charged up to 5 V vs. K^+/K.

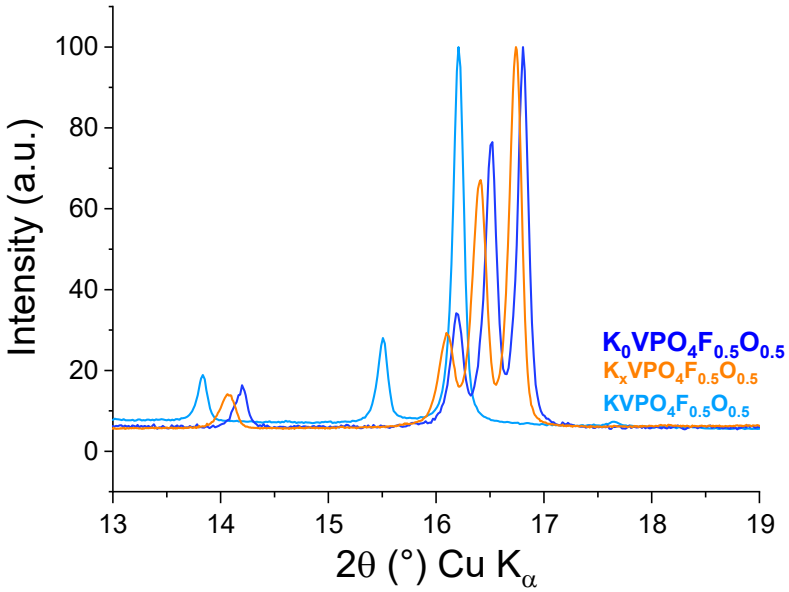

Figure S9: XRD patterns of the first four Bragg reflections for pristine $KVPO_4F_{0.5}O_{0.5}$, chemically deintercalated $K_0VPO_4F_{0.5}O_{0.5}$, and electrolyte exposed $K_xVPO_4F_{0.5}O_{0.5}$.

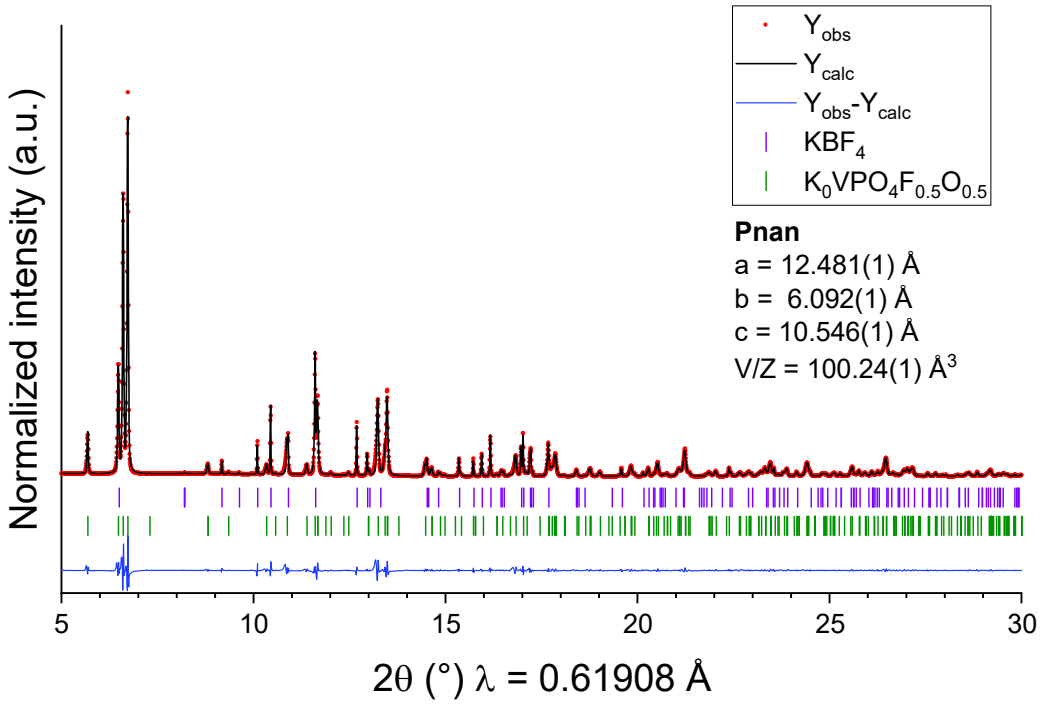

Figure S10: Full pattern matching refinement of chemically deintercalated $KVPO_4F_{0.5}O_{0.5}$, showing two phases $K_0VPO_4F_{0.5}O_{0.5}$ and KBF_4.